JOURNAL OF SPACECRAFT AND ROCKETS
Vol. 34, No. 1, January–February 1997

# U-Groove Aluminum Weld Strength Improvement

V. Verderaime* and R. Vaughan*
*NASA Marshall Space Flight Center, Huntsville, Alabama 35812*

**Though butt-welds are among the most preferred joining methods in aerostructures, their strength dependence on inelastic mechanics is generally the least understood. This study investigated experimental strain distributions across a thick aluminum U-grooved weld and identified two weld process considerations for improving the multipass weld strength. One is the source of peaking in which the extreme thermal expansion and contraction gradient of the fusion heat input across the groove tab thickness produces severe angular distortion that induces bending under uniaxial loading. The other is the filler strain hardening decreasing with increasing filler pass sequences, producing the weakest welds on the last weld pass side. Both phenomena are governed by weld pass sequences. Many industrial welding schedules unknowingly compound these effects, which reduce the weld strength. A depeaking index model was developed to select filler pass thickness, pass numbers, and sequences to improve depeaking in the welding process. The result was to select the number and sequence of weld passes to reverse the peaking angle such as to combine the strongest weld pass side with the peaking induced bending tension component side to provide a more uniform stress and stronger weld under axial tensile loading.**

## Nomenclature

$E$ = elastic modulus, ksi
$F$ = material strength, ksi
$H$ = specimen thickness, in.
$h$ = weld pass thickness, in.
$K$ = inelastic strength coefficient, ksi
$M$ = induced moment, in.-kips
$m$ = weld sequence number
$N$ = applied axial load, kips
$n$ = strain-hardening exponent, total number of weld passes
$T$ = temperature, °F
$t$ = U-groove tabs thickness, in.
$w$ = specimen width, in.
$\alpha$ = coefficient of thermal expansion, in./in./°F
$\phi$ = peaking angle, rad

*Subscripts*

$e$ = elastic variable
$i$ = strain gauge number, weld pass series
$j$ = weld pass number
$k$ = designated temper
$M$ = moment variable
$N$ = axial load variable
$p$ = inelastic variable
tu = tensile ultimate
ty = tensile yield
$\alpha$ = thermal variable

## Introduction

As structural environments and component sizes increase, butt-weld thicknesses increase, weld development and processes become more complex, and joint strengths are less predictable. One early study modeled a uniaxial butt-weld specimen having different inelastic lateral contraction rates between preweld material and weld filler and discovered a metallurgical discontinuity at the interfaces.[1] Discontinuity stresses, especially transverse shear, were later experimentally verified on a thick weld cross section in uniaxial test.[2] The primary objective of the reported study was to further explore the multipass welding process and resulting structural properties of weld filler passes from experimental test data[3] and to identify weld process variables that should improve strength performance.

## Weld Peaking Specimen

The aluminum test specimen shown in Fig. 1 was a 0.71 in. wide slice from a double U-grooved butt weldment of two very large machined 2219 aluminum panels. The weld filler was 2319 aluminum with the beads ground off. The panels were 1.4 in. thick, and the butted tab thickness between the double U grooves was 0.375 in. It was tungsten inert gas welded using the symmetrical welding schedule noted in Fig. 1, referred to as a normal welding schedule. The butted tabs were tacked and then continuous fusion welded from the same side, incurring a net initial peaking angle $\phi_2$. Weld peaking is an unintentional angular panel displacement resulting from weld thermal gradient strain. Subsequent welds were filler passes serially applied, first in the groove opposite passes 1 and 2 and then on the reverse side groove, for a total of eight passes.

Weld pass 1 (Fig. 1) was crucial to the butted edge mismatch. In this weld pass, the double U-groove tabs at the midplane were butted, the panel surface planes were aligned, the assembly was constrained, and the butted tabs were fusion tack welded (without filler material) on one side. The tack weld pass produced local thermal expansion on the butted tabs and was followed by cooling contraction. The cooling induced a tensile strain on the tack weld side and compression on the unfused side of the tab, which mildly peaked the panels with the obtuse angle on the tack welded (pass 1) side.

The intense weld heat input from pass 2 severely increased the adverse peaking angle. It was another fusion weld pass applied continuously on the same side of the tack weld, and it had the highest heat input rate to fuse the total tab thickness. The associated extreme thermal expansion and contraction gradient across the tab thickness produced the maximum peaking angle in the process with the obtuse angle again on the heat source (pass 1) side.

The next three passes were weld filler passes (thinner than the tabs) requiring less heat and were applied in the groove opposite the

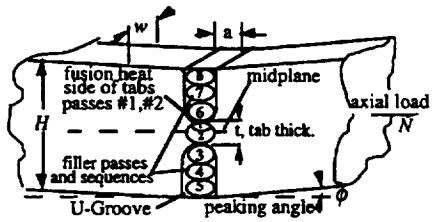


**Fig. 1 Test specimen configuration.**

Received Feb. 15, 1996; revision received Sept. 25, 1996; accepted for publication Sept. 30, 1996. 

*Aerospace Engineer, Structures and Dynamics Laboratory.

tack pass 1 side. Each weld pass produced a thermal gradient and expansion across the welded section. Upon cooling, the filler pass contracted inelastically and then elastically in tension, which bent and strain hardened the tabs and the built-up filler passes. These passes reduced the peaking angle (depeaking) produced by the two fusion weld passes. Subsequent weld filler passes were applied on the opposite groove, producing less thermal straining and moderately increasing the weld peaking.

## Depeaking Model

The extent of peaking at any point in the process depended on the initial peaking from the fusion passes and the depeaking and peaking contributions of successive filler weld passes. Increasing the laid-up weld thickness increases the section modulus, which stiffens and reduces the panel deflection rate induced by the succeeding thermally contracted filler passes. It then follows that successive thermal bending and strain hardening decrease and that the net depeaking angle is governed by the groove side accumulating the most and earliest thermal tensile straining. Therefore, the peaking angle $\phi_m$, for any pass $j > 2$ and at the $m$th sequence in the welding process may be expressed by

$$\phi_m = \phi_2 + \sum_{j=3}^{m} s_j \phi_j \tag{1}$$

where the first term is the initial peaking angle ($\phi_2 > \phi_3$) produced by the fusion welds on the U-groove tabs. The second term is the sum of subsequent depeaking and peaking weld passes for $j \geq 3$. The coefficient $s$ polarizes the weld pass sequence, where $s = +1$ refers to the peaking weld pass applied in the groove on the weld pass 1 side of the specimen and $s = -1$ refers to the depeaking pass applied in the opposite groove.

Figure 2 qualitatively models the weld peaking behavior of the $j$th pass in the welding process. The peaking angle $\phi$ at the $j$th weld pass was derived with designer control variables, which are the weld pass thicknesses $h_i$, the polarity, and the accumulated thickness. Passive control variables, such as material constants and unique coefficients, were lumped into unquantified coefficients leading to versatile qualitative expressions.

The cooling contraction of the $j$th weld pass induces a tensile force of

$$f_j = \sigma_\alpha h_j \tag{2}$$

where the thermal stress is derived from the filler thermal contraction equated to the stress tension displacement,

$$\Delta = a\alpha T = a(\sigma_\alpha / E)$$

and is reduced to

$$\sigma_\alpha = \alpha E T \tag{3}$$

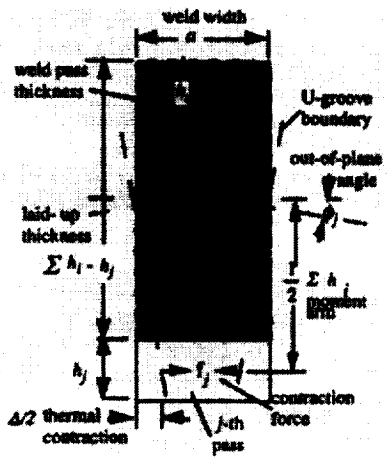


**Fig. 2 Peaking from $j$th filler pass.**

Substituting Eq. (3) and the moment arm in Fig. 2 into Eq. (2), the moment imposed by the thermal contraction force about the accumulated weld passes centroid is

$$M_j = f_j s_j \left[\frac{1}{2}\sum_2^j h_i\right] = \frac{1}{2}\alpha E T s_j h_j \sum_2^j h_i \tag{4}$$

and the resulting peaking angle of the stub filler section was approximated by a third-degree stress function[4]:

$$\phi_j = \frac{c_1 M_j \alpha}{E\left(\sum_2^j h_i - h_j\right)^3} \tag{5}$$

Substituting Eq. (4) into Eq. (5), the peaking angle induced by the $j$th weld pass is

$$\phi_j = \frac{c s_j h_j \sum_2^j h_i}{\left(\sum_2^{j-1} h_i\right)^3} \tag{6}$$

Substituting Eq. (6) into the second term of Eq. (1), the depeaking angle at the end of the $m$th sequence is given by

$$\phi_{m>2} = \phi_m - \phi_2 = \sum_{j=3}^{m} s_j \phi_j = c_\alpha Z_{m>2}$$

where the desired depeaking index is expressed by

$$Z_{m>2} = \sum_{3}^{m} \frac{s_j h_j \sum_2^j h_i}{\left(\sum_2^{j-1} h_i\right)^3} \tag{7}$$

The depeaking index of Eq. (7) was applied to the normal welding schedule of Fig. 1, having a uniform filler weld pass thickness in inches of

$$h_i = \frac{(H - t)}{n - 2} = \frac{(1.4 - 0.375)}{8 - 2} = 0.17$$

Substituting the uniform filler thickness into Eq. (7), the depeaking index after the $m = 5$ pass is

$$Z_5 = -\frac{0.17(0.375 + 0.17)}{(0.375)^3} - \frac{0.17[0.375 + 2(0.17)]}{(0.375 + 0.17)^3}$$

$$- \frac{0.17[0.375 + 3(0.17)]}{[0.375 + 2(0.17)]^3} = -3.3$$

and after $m = n = 8$ is

$$Z_8 = Z_5 + 0.56 = -2.7$$

Depeaking indices after each filler pass are listed in Table 1 for centered tabs and for a normal weld schedule. Because the specimen showed a peaking angle of 0.02 rad, the peaking index may be assumed to be $Z_2 > +2.8$ and the normal weld schedule proved to be insufficient. In another case, the U-groove tabs were assumed to be machined off centered by a distance equal to one pass of the same filler thickness to provide an additional depeaking weld pass opposite the obtuse angle side and within the specimen thickness. The depeaking index increased to $-3.3$, which might have reversed the weld peaking side.

Other weld schedule options with centered tabs were assessed through Eq. (7). Increasing the welds to four thinner filler passes than the normal weld schedule on the peaking side for a total of seven filler passes and two fusion welds provided an index of $-2.8$ and no improvement over the normal weld schedule. Increasing the

**Table 1 Depeaking indices at weld sequences**

| Weld sequence, $m$ | 3 | 4 | 5 | 6 | 7 | 8 |
|---|---|---|---|---|---|---|
| Centered tab, $Z$ | −1.7 | −2.5 | −3.3 | −3.1 | −2.9 | −2.7 |
| Off-centered tab, $Z$ | −1.7 | −2.5 | −3.3 | −3.6 | −3.4 | −3.3 |

weld passes to eight uniform filler thickness provided a worse index of −1.9.

## Weld Test Data

The complex thermal straining, work hardening, and annealing environments experienced by each unique weld pass posed the question of how unique their structural properties might be after the final heat treatment. Reference 3 provided the necessary experimental strain data of the Fig. 1 specimen and as instrumented in Fig. 3. A total of five equidistant electrical strain gauges were oriented to obtain axial strain measurements along the specimen thickness under uniaxial loading.

Surface mounted gauges 1 and 5 measured strains from weld passes 8 and 5, respectively, of the normal welding schedule. Gauges 2, 3, and 4 measured average strains from pairs of weld passes 7 and 6, 1 and 2, and 3 and 4, respectively. Table 2 provides the experimental strain gauge data[3] as a function of incrementally applied axial loads.

Figure 4 illustrates the measured strain distributions along the weld filler cross section, using Table 2 data. At loads less than 15 kips, strains are seen to produce planes of uniformly varying strains along the cross section that are indicative of elastic bending of a homogeneous material. Inelastic strain responses are spotted by the onset change of constant strain rate to a suddenly increased rate under constant loading rate. The inelastic strains are noted to not conform into planes for common steps of axial loading, which clearly denotes zones of nonhomogeneous filler materials. This onset of inelastic strain behavior of each weld pass under constant load rate signifies a unique filler pass property, which may be estimated from materials and load equilibrium models.

**Table 2 Experimental weld strains, $10^{-3}$ in./in.**

| | Loads $N$, kips | | | | | | |
|---|---|---|---|---|---|---|---|
| Gauge | 5 | 10 | 15 | 20 | 25 | 30 | 35 |
| 1 | 0.8 | 1.5 | 2.6 | 4.0 | 6.3 | 10.4 | 19.0 |
| 2 | 0.5 | 1.0 | 1.6 | 2.4 | 3.4 | 5.6 | 11.8 |
| 3 | 0.4 | 0.9 | 1.4 | 2.0 | 2.8 | 4.0 | 7.0 |
| 4 | 0.4 | 0.8 | 1.3 | 1.8 | 2.6 | 3.7 | 7.0 |
| 5 | 0.4 | 0.6 | 1.0 | 1.2 | 1.6 | 2.0 | 3.2 |

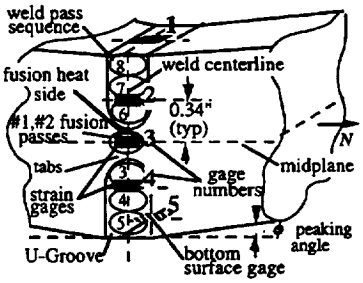


**Fig. 3 Strain instrumentation.**

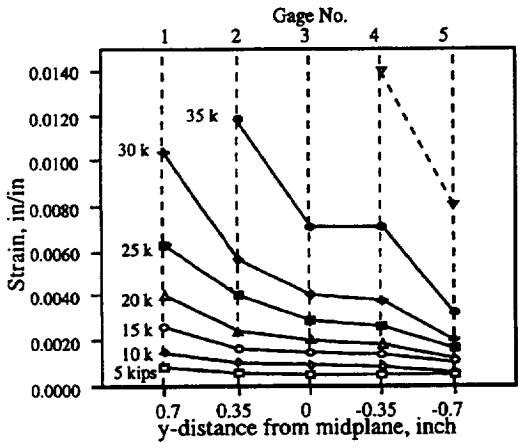


**Fig. 4 Strain distribution across thickness.**

## Weld Filler Properties

Modeling elastic–inelastic behavior could be very difficult unless idealized into the simplest mathematical expressions within the physical phenomena of the material and its application.[5] The uniaxial stress–strain relationship of a polycrystalline material may be appropriately represented by the power expression[6]

$$\sigma = K\varepsilon^n \tag{8}$$

requiring no interpretation through theory. The strain-hardening exponent $n$ is the log-log slope of Eq. (8) and is defined by $n = 1$ in the elastic region when $\sigma \leq F_{ty}$.

Many mechanical properties of aluminum are seen to be related by their common face-centered-cubic lattice substructure and copper alloy. They all have a common elastic modulus of $E = 10{,}500$ ksi, and all demonstrate similar strain-hardening curves. Their strength dispersions are fixed by their temper processes, which establish their unique elastic stress limit and strain-hardening slope. Therefore, it is not surprising that the inelastic stress–strain slopes of any temper $k$ are noted to vary linearly with yield stresses.[7]

Given the yield stress of any temper, the strain-hardening exponent (slope) may be shown to be approximated (within 5%) by the linear expression

$$n_k = 0.34 - 0.0045F_{ty,k} \tag{9}$$

The strength coefficient $K$ is evaluated at the elastic–inelastic material interface, which is the yield stress, and the coefficient is expressed by

$$K = E^n F_{ty}^{(1-n)} \tag{10}$$

Thus, determining the experimental yield stress, the Eq. (8) inelastic parameter of each weld pass may be derived through Eqs. (9) and (10).

Because of peaking induced bending, the onset of yield strain is a serendipity observed in Fig. 4 to emerge at one gauge per each sequentially and successively increased interval of axial loading. Then, for each interval of applied loading, the portion of that load imposed on each gauge region is expressed by the product of that proportional area and Eq. (8) with the measured strain. Their sum for that interval is equated to the external–internal load equilibrium formula

$$N = wh\sum K\varepsilon_p^n p + E\sum \varepsilon_e p \tag{11}$$

from which each material set of parameters is calculated through Eqs. (9) and (10) through each increasing interval of applied loading.

Terms on the right of the equation are the sum of inelastic and elastic internal loads calculated from their measured strains, respectively. The weld pass thickness was assumed to be equally divided along the thickness for an average of $h = H/8 = 0.175$ in., and $p$ is the number of passes represented by each respective strain gauge. This technique was applied to data from all five strain gauges to identify and define weld pass inelastic properties along the weld centerline.

In determining filler properties from strains induced at load $N = 15$ kips, at least one strain had to be inelastic to not exceed the load equilibrium of Eq. (11). That inelastic strain had to be on the verge of a strain rate increase, such as gauge 1 measuring $\varepsilon_1 = 0.0026$. Substituting the inelastic and all elastic strains induced at $N = 15$ kips into Eq. (11),

$$pK(0.0026)^n = \frac{15}{0.124} - 10{,}500[0.001 + 2(0.0016 + 0.0014 + 0.0013)]$$

where $p = 1$, the inelastic stress in kilopounds per square inch was

$$K(0.0026)^n = 20.2 \tag{12}$$

By trial (or Newton method), a yield stress was selected and applied into Eqs. (9) and (10) to satisfy Eqs. (8) and (12). Resulting properties representing weld pass 8 are listed in Table 3. At 20-kips

**Table 3 Weld filler inelastic properties**

| Gauge: | 1 | 2 | 3 | 4 | 5 |
|---|---|---|---|---|---|
| Weld pass: | 8 | 7.6 | 1.2 | 3.4 | 5 |
| $F_{ty}$, ksi | 19 | 22 | 27 | 37 | 30 |
| $n$ | 0.245 | 0.241 | 0.218 | 0.174 | 0.205 |
| $K$, ksi | 94.7 | 97.3 | 99.3 | 98.6 | 99.7 |
| $\sigma_{tu}$, ksi | 46 | 49 | 53 | 58 | 56 |
| $\varepsilon_{ty}$ | 0.0018 | 0.0021 | 0.0025 | 0.0035 | 0.0028 |

loading, the inelastic weld pass properties to be determined were passes 6 and 7 represented by gauge 2. Substituting the derived inelastic properties of weld pass 8 in Eq. (8) and continuing as with the 15-kips loading case, the load equilibrium of Eq. (11) was

$$2K(0.0024)^n = \frac{20}{0.124} - 94.7(0.004)^{0.254} - 10{,}500[0.0012 + 2(0.002 + 0.0018)]$$

and the inelastic stress was $K(0.00224)^n = 22.8$ ksi.

Results from similarly derived inelastic properties at all other strain gauges along the weld centerline are also listed in Table 3. Though listed results from Eq. (11) confirmed the suspected variation of inelastic properties among the weld passes, the orderly decrease of filler yield stress unexpectedly correlated with the orderly increase in weld pass sequence. The last weld pass 8 at gauge 1 was noted to have the lowest yield property, the prior pass had the next lowest yield property, and so forth. This phenomenon was verified by an independent graphic analysis, producing the same results.

Decreasing filler pass yield stress with increasing weld pass sequence is a particularly interesting phenomenon in that it coincides with the decreasing peaking index of Eq. (7). Because weld depeaking and strain hardening decreases with increasing passes, later filler passes experience less strain hardening and, therefore, result in a lower yield stress. Consequently, if the last pass filler, which is weakest and is on the obtuse angle side of the specimen, is combined with the tension component of the induced moment, the compounded tension on the last pass filler will prematurely rupture under axial loading.

A more significant weld strength improvement would be to depeak the weld sufficiently to reverse the obtuse angle on the first pass side to induce the tension component of the peaking moment on the earlier passes having higher yield stresses and strength. This process would provide a more uniform stress across the weld thickness, producing a stronger weld in axial tension.

## Summary and Conclusions

Weld fillers, having the lowest elastic limit and limited width (gauge length), will yield first and progressively distort most in bending. This principle was especially appreciated in observed weld strength reduction of multipass welds leading to this study on the influences of peaking.

A depeaking index model was developed for a double U-grooved weldment that denoted the groove side receiving the thicker and most filler passes earliest produced the greater depeaking angle. A large range of depeaking angles may be achieved through the welding process selection of designer control parameters, such as filler pass thickness, number of passes, and polarities.

Using experimental strain data from a double U-groove aluminum weldment, the filler pass inelastic properties were noted to vary across the weld thickness with the weld filler yield stress decreasing with increasing sequence number. This phenomenon coincided with the decreasing peaking index model, in which strain hardening decreases with increasing passes, and the resulting weaker last pass filler (obtuse angle side of the specimen) combines with the tension component side of the induced bending to prematurely rupture under uniaxial loading.

An enhanced welding schedule would depeak the weld sufficiently to reverse the obtuse angle to the first pass side to impose the tension component of the induced bending on the earlier weld passes having higher yield and ultimate strengths. Reversing the weld peaking provides a more uniform and lower stress across the weld thickness, resulting in a stronger tensile joint. This simple innovation may be the least intrusive modification on current and future structural productions.

## Acknowledgments

The authors appreciate the review comments by Dennis Moore and are grateful to James Blair for this assigned opportunity and for his remarks and usual professional support.

## References

[1]Verderaime, V., "Plate and Butt-Weld Stresses Beyond Elastic Limits," NASA TP-3075, Jan. 1991.

[2]Kerkof, S., "AFT Skirt Weld Analysis Methods," United Technology, United Space Boosters, Inc., presentation to Marshall Space Flight Center, AL, April 1991.

[3]Gambrell, S., "Use of Photostress and Strain Gages to Analyze Behavior of Weldments," NASA/MSFC Contract NAG 8-293, Sub 93-101, Univ. of Alabama, Tuscaloosa, AL, April 1993.

[4]Timoshenko, S., and Goodier, J., *Theory of Elasticity*, 2nd ed., McGraw–Hill, New York, 1951, Chap. 3.

[5]Phillips, A., *Introduction to Plasticity*, 2nd ed., Ronald Press, 1956, Chap. 3.

[6]Dieter, G., *Mechanical Metallurgy*, 3rd ed., McGraw–Hill, New York, 1986, Chap. 4.

[7]Anon., "Metallic Materials and Elements for Aerospace Vehicle Structures," U.S. Dept. of Defense, MIL-Handbook C5, 1976, Chap. 3.

R. B. Malla
*Associate Editor*